RF Band-Pass Sampling Frontend for Multiband Access CR/SDR Receiver

HyungJung Kim, Jin-up Kim, JaeHyung Kim, Hongmei Wang, and InSung Lee

Radio frequency (RF) subsampling can be used by radio receivers to directly down-convert and digitize RF signals. A goal of a cognitive radio/software defined ratio (CR/SDR) receiver design is to place the analog-to-digital converter (ADC) as near the antenna as possible. Based on this, a band-pass sampling (BPS) frontend for CR/SDR is proposed and verified. We present a receiver architecture based second-order BPS and signal processing techniques for a digital RF frontend. This paper is focused on the benefits of the second-order BPS architecture in spectrum sensing over a wide frequency band range and in multiband receiving without modification of the RF hardware. Methods to manipulate the spectra are described, and reconstruction filter designs are provided. On the basis of this concept, second-order BPS frontends for CR/SDR systems are designed and verified using a hardware platform.

Keywords: RF subsampling, band-pass sampling, cognitive radio (CR), software defined ratio (SDR), mutliband access.

Manuscript received Sept. 15, 2009; revised Dec. 18, 2009; accepted Jan. 4, 2010.

This work was supported by the IT R&D program of Ministry of Knowledge and Economy of Republic of Korea and Institute for Information Technology Advancement under project 2008-F-001-02.

HyungJung Kim (phone: +82 42 860 3811, email: acekim@etri.re.kr) and Jin-up Kim (email: jukim@etri.re.kr) are with the Internet Research Laboratory, ETRI, Daejeon, Rep. of Korea.

JaeHyung Kim (email: hyung@changwon.ac.kr) and Hongmei Wang (email: iwanghongmei99@163.com) are with the School of Mechatronics Engineering, Changwon National University, Changwon, Rep. of Korea.

InSung Lee (email: inslee@chungbuk.ac.kr) is with the School of Electrical, Electronics and Computer Engineering, Chungbuk National University, Cheongju, Rep. of Korea.

doi:10.4218/etrij.10.1409.0073

I. Introduction

Cognitive radio (CR) technology can theoretically interoperate among incompatible communication systems. In other words, cognitive radio is a radio function that is capable of switching from a crowded part of the radio frequency spectrum to a radio frequency region that is more sparsely populated but can still receive the original signals of interest [1]-[2]. Also, software defined radio (SDR) is programmable radio whose functions are extensively defined in software and thus can support multistandard or multiband radio communications [3]. As a requirement for CR/SDR, a wideband analog frontend (FE) and analog-to-digital converter (ADC) are necessary to allow signals from different systems to be processed [4].

In radio receivers, complete implementation of the CR/SDR concept is mainly limited by the frontend. Building flexible frontends in classic ways is challenging because of the narrow bandwidth of intermediate frequency (IF) filters and the frequency range of synthesizers [5], [6]. The key to CR/SDR is the placement and design technique of the ADC in the channel processing stream, and the goal is to put the ADC as close as possible to the antenna [7].

RF band-pass sampling (BPS) is a solution for CR/SDR which provides a frontend with maximum flexibility [8]. The sampling frequency requirement is no longer based on the frequency of the RF carrier but rather on the information bandwidth of the signal. This makes it possible to have an interface between the RF stage and the ADC in a radio receiver frontend. The process of BPS samples a signal at the RF stage and shifts to a near baseband stage through intentional aliasing. This technique can be used immediately on a modulated band-pass signal with the sampling rate of only twice the information

bandwidth, which is much less than the Nyquist rate. Therefore, the BPS technique provides an interface between the RF stage and ADC, and also gives a wide choice of sampling rates for a multimode or multiband radio design [9], [10]. Another advantage of BPS is that the proper choice of sampling frequency enables simultaneous down-conversion of multiband signals.

In this paper, we present a second-order BPS method to design an FE that can realize universal access or spectrum scanning in a wide frequency band range and the implementation of a hardware platform to verify its performance. This second-order BPS receiver can also be utilized as an FE for simultaneous multiband access to a wide range of frequencies with only a reconfiguration. In section II, a method for universal access to arbitrary bands using the second-order BPS method is described. Section III describes a second-order BPS receiver and signal processing technique for multiband access. Section IV describes the implementation and performance test results of the hardware platform. Finally, we provide a conclusion in section V.

II. Second-Order BPS Method and Universal Access

1. Second-Order BPS

Denoting the RF filter's bandwidth as B, an RF band-pass signal $R(f)$ is sampled by using a sampling rate of f_s=2B. Any signal in the frequency zone of index n is expressed by

$$(n-1/2)f_s < |f| < (n+1/2)f_s \qquad (1)$$

and is aliased into the first Nyquist zone $|f| < B$.

In a second-order BPS receiver, two ADCs (referred to as ADC A and ADC B) produce streams A and B, respectively. The second ADC (ADC B) operates with delay T_Δ during the sampling time; hence, it introduces a relative phase difference between the two ADC sample streams, A and B. Let us define the spectra of sample data in streams A and B as $R_A(f)$ and $R_B(f)$, respectively. These two spectra satisfy the following expression as presented in [9]:

$$R_B^\delta(f) = R_A^\delta(f)\cdot e^{-j2\pi T_\Delta f_s} = R_A^\delta(f)\cdot\beta^n, \qquad (2)$$

where n denotes the index of the frequency band position in (1), and $\beta = e^{-j2\pi T_\Delta f_s}$.

In Fig. 1, we depict some examples of RF signals in the same frequency zone that will be repositioned within $|f| < B$ with the same phase shift in stream B when we select the sample rate as f_s=2B. The positive frequency spectrum of $R(f)$ is defined as $R_+(f)$, and the negative frequency spectrum is $R_-(f)$. The spectra of streams A and B are denoted by $R_A^\delta(f)$ and $R_B^\delta(f)$, respectively. The images from both sides interfere

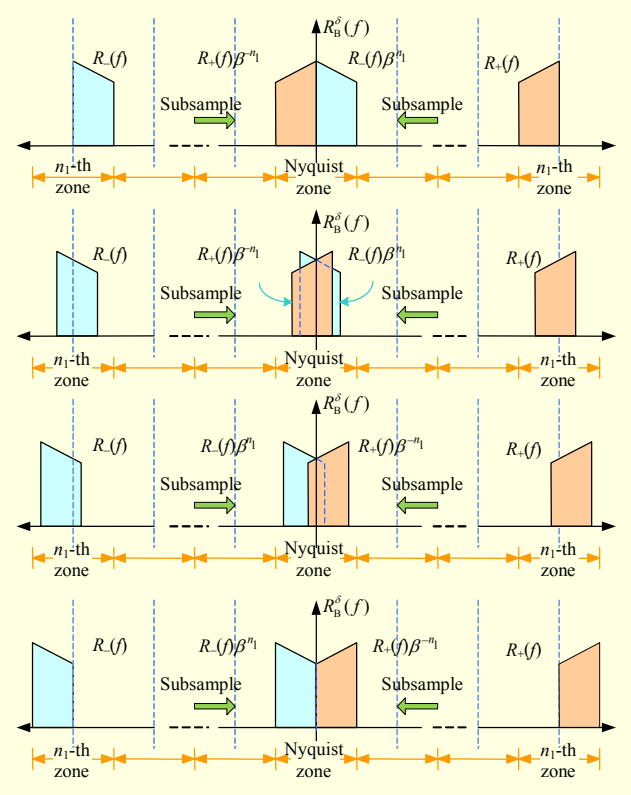

Fig. 1. RF signals and their subsampled spectra in stream B.

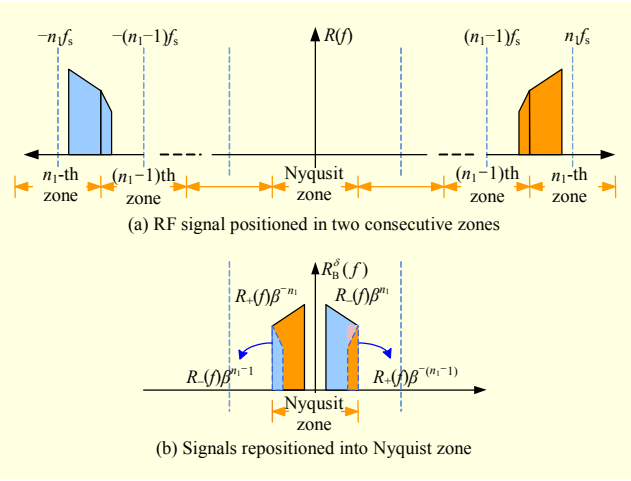

Fig. 2. Non-integer positioned RF signal and subsampled signal spectrum.

with each other. Note that all these cases have the same relative phase between streams A and B because the zone index is same. This implies that the same interpolant filter is used to remove self images.

This BPS method is not restricted to an integer-positioned RF signal. Thus, a signal spectrum may occupy two consecutive frequency zones as depicted in Fig. 2. As shown in Fig. 2(b), two segments of the RF spectrum are repositioned in

the positive and negative side of the Nyquist zone, but they have different phase shifts. Due to the phase difference between the two images, and therefore, by proper design of the interpolant filters of the two streams that manipulate spectra in $|f|<B$, either $R_{+}(f)$ or $R_{-}(f)$ can be reconstructed without interference.

2. Reconstruction Filters

Spectrum sensing used to identify unused segments is a key requirement of CR. The universal access BPS architecture described in this section provides an effective method to scan a wide range of frequencies.

- The sampling rate is fixed at $f_s=2B$.
- It has a tunable RF filter with bandwidth B.
- The spectrum can be down-converted and is identifiable as being integer positioned or not.

Two different types of reconstruction filters are required for the signals positioned within a single zone and across two zones. We present the frequency response of the reconstruction filter in the next subsections.

A. Reconstruction Filter for an RF Signal Occupying One Frequency Zone

To eliminate overlapped images, reconstruction filter $S_A(f)$ and $S_B(f)$ are applied to streams A and B, respectively. The spectrum of the recovered signal is expressed by

$$R^{\delta}(f)=S_A(f)\cdot R_A^{\delta}(f)+S_B(f)\cdot R_B^{\delta}(f). \tag{3}$$

By separating the positive frequency region from the negative frequency region of the spectrum, (3) becomes

$$R^{\delta}(f)=S_A(f)\cdot[R_{+A}^{\delta}(f)+R_{-A}^{\delta}(f)]+S_B(f)\cdot[R_{+B}^{\delta}(f)+R_{-B}^{\delta}(f)]. \tag{4}$$

Here, $R_{+}(f)$ is reconstructed by eliminating $R_{-}(f)$, if $S_A(f)$ and $S_B(f)$ satisfy

$$\begin{aligned} B\cdot[S_A\cdot R_{+A}^{\delta}(f)+S_B\cdot R_{+B}^{\delta}(f)]&=CR_{+A}(f-2n_1B),\\ B\cdot[S_A\cdot R_{-A}^{\delta}(f)+S_B\cdot R_{-B}^{\delta}(f)]&=0, \end{aligned} \tag{5}$$

where C is an arbitrary complex constant.

For convenience, we select $S_A(f)$ in its simplest form as

$$S_A(f)=\begin{cases}\dfrac{1}{B}, & |f|<B,\\ 0, & \text{otherwise},\end{cases} \tag{6a}$$

$$S_A(t)=\frac{2\sin(\pi f_s t)}{\pi f_s t}. \tag{6b}$$

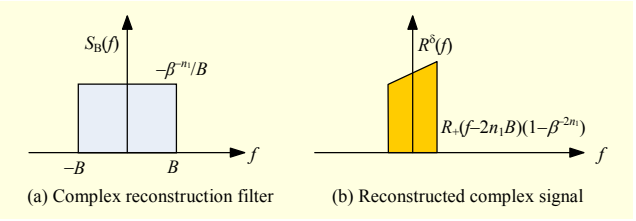

(a) Complex reconstruction filter (b) Reconstructed complex signal

Fig. 3. Reconstruction filters and recovered signal spectrum.

By substituting (6) into (5), $S_B(f)$ is obtained by

$$S_B(f)=\begin{cases}\dfrac{-\beta^{-n_1}}{B}, & |f|<B,\\ 0, & \text{otherwise},\end{cases} \tag{7a}$$

$$S_B(t)=-\frac{2e^{j2\pi f_s T_A n_1}\sin(\pi f_s t)}{\pi f_s t}. \tag{7b}$$

Here, $S_A(f)$ is a simple real value gain, but $S_B(f)$ is a complex filter as shown in Fig. 3(a). As the maximum bandwidth of $S_A(f)$ and $S_B(f)$ is B, and because a sampling rate of $f_s=2B$ is used, digital filters are implemented by sampling the inverse transforms given by (6b) and (7b). The reconstructed complex signal is depicted in Fig. 3(b).

B. Reconstruction Filter for an RF Signal Occupying Two Consecutive Frequency Zones

For reconstruction of complex signal $R_{+}(f)$ in Fig. 2, (5) is used again to derive $S_A(f)$ and $S_B(f)$. If $S_A(f)$ is selected as (6), $S_B(f)$ is given by

$$S_B(f)=\begin{cases}-\beta^{-(n_1-1)}/B, & -B<f<0,\\ -\beta^{-n_1}/B, & 0\le f<B,\end{cases} \tag{8a}$$

$$S_B(t)=\frac{je^{j\pi f_s(2T_A(n_1-1)-t)}(e^{j\pi f_s t}-1)(e^{j\pi f_s(2T_A+t)}+1)}{\pi f_s t}. \tag{8b}$$

The reconstruction filter and resulting spectrum of reconstructed samples are depicted in Figs. 4(a) and 4(b), respectively. In most cases, a complex frequency shift is required to align the signal spectrum between 0 and B.

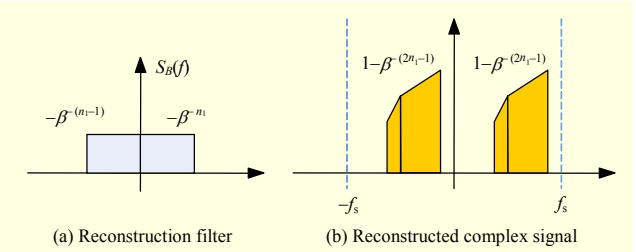

(a) Reconstruction filter (b) Reconstructed complex signal

Fig. 4. Reconstruction filters and recovered signal spectrum.

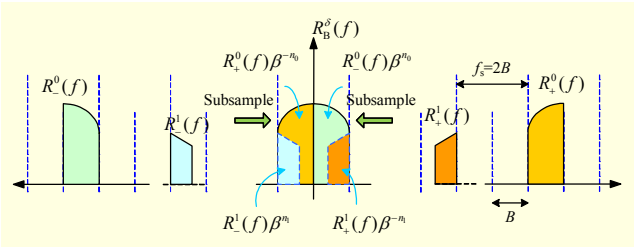

Fig. 5. Spectrum of stream B when two bands are down-converted simultaneously.

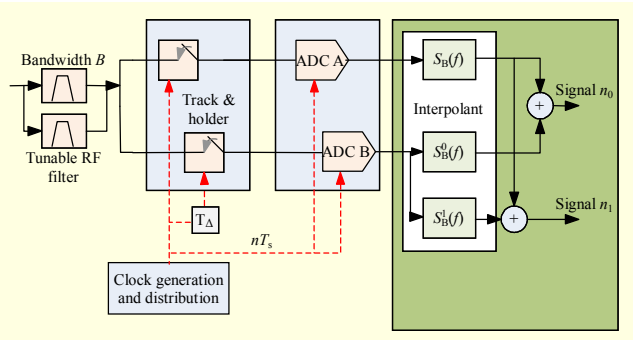

Fig. 6. BPS receiver architecture for environment sensing.

III. Frontend Architecture for Multiband Receiver

A simultaneous down-conversion function of more than two signals is required in CR systems. We introduce a second-order BPS technique that realizes multiband receiving and environment sensing. By proper design of the interpolant and taking full advantage of digital filters, multiband signals may be received simultaneously and separated.

1. Second-Order BPS FE for Two-Band Signals

In subsection 2, we described a second-order BPS method to monitor or receive signals in a fixed bandwidth of B at each scanning trial. The same architecture allows the environment to be sensed by scanning the broadband range of spectrum while receiving a fixed spectrum for a normal channel. To do this we set the following preconditions:

- Two tunable RF filters with bandwidth B are used.
- The ADCs operate at a sampling-rate of f_s=2B.
- The frequency region is divided into segments of bandwidth B.
- The pass-band of tunable RF filters is forced to be aligned with the segment boundary.

The third and fourth conditions ensure that the reconstruction filters always separate two bands without interference. If the condition is not met, the amount of mutual interference depends on the band positions.

First, a channel for normal receiving is selected in one of the frequency segments, and the second RF filter then scans other segments dynamically. The frequency response of stream B, in which two bands are down-converted simultaneously by second-order BPS, is depicted in Fig. 5. It is assumed that $R^0(f)$ and $R^1(f)$ are two RF signals in the frequency zones n_0 and n_1, respectively.

2. Image Rejection Filter Design

Two signals are separated by designing proper digital filters. The environment sensing receiver can utilize this feature provided by the same second-order BPS frontend described in section II. The BPS receiver architecture for environment sensing is proposed and shown in Fig. 6.

The three interpolants in Fig. 6 are reconfigurable FIR filters which are designed to remove mutual images as shown in Fig. 5. For example, interpolants $S_A(f)$ and $S_B^0(f)$ are designed to recover $R^0(f)$ while $R^1(f)$ is suppressed. Therefore, interpolants $S_A(f)$ and $S_B^0(f)$ should satisfy the following in $|f| \le B$:

$$\begin{aligned} B\cdot[S_A\cdot R_{+A}^{\delta,0}(f)+S_B^0\cdot R_{+B}^{\delta,0}(f)] &= CR_{+A}^0(f-2n_0B),\\ B\cdot[S_A\cdot R_{-A}^{\delta,0}(f)+S_B^0\cdot R_{-B}^{\delta,0}(f)] &= CR_{-A}^0(f+2n_0B), \end{aligned} \tag{9a}$$

and

$$\begin{aligned} B\cdot[S_A\cdot R_{+A}^{\delta,1}(f)+S_B^0\cdot R_{+B}^{\delta,1}(f)] &= 0,\\ B\cdot[S_A\cdot R_{-A}^{\delta,1}(f)+S_B^0\cdot R_{-B}^{\delta,1}(f)] &= 0, \end{aligned} \tag{9b}$$

where $R^{\delta,0}(f)$ and $R^{\delta,1}(f)$ stand for the spectra of subsampled signals of RF signals $R^0(f)$ and $R^1(f)$, respectively.

Again for simplicity, $S_A(f)$ is selected as in (6). Thus, $S_B^0(f)$ is derived by solving (9a) and (9b) simultaneously:

$$S_B^0(f)=\begin{cases}\dfrac{-\beta^{n_1}}{B}, & -B<f<0,\\[2ex] \dfrac{-\beta^{-n_1}}{B}, & 0<f<B.\end{cases} \tag{10}$$

To reconstruct $R^1(f)$ simultaneously, another interpolant $S_B^1(f)$ is designed in the same manner as that in (9a) and (9b):

$$S_B^1(f)=\begin{cases}\dfrac{-\beta^{-n_0}}{B}, & -B<f<0,\\[2ex] \dfrac{-\beta^{n_0}}{B}, & 0<f<B,\end{cases} \tag{11}$$

As the frequency segments are divided by bandwidth B, two selected signals could be included in the same frequency zone. There are no overlapped images having the same phase shift, but two signals are extracted simultaneously in any case by a

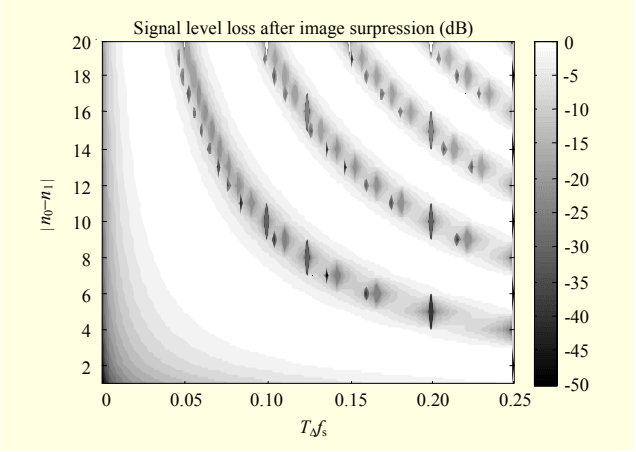

Fig. 7. Relative signal strength of recovered signal.

proper design of $S_B^0(f)$.

The envelope of the recovered signal is expressed by (12). From (12), it is expected that the recovered level of the desired signal varies periodically as a function of $T_\Delta f_S |n_1 \pm n_0|$. Figure 7 shows the relative signal strength of a recovered signal in a decibel scale.

Given $|n_1 \pm n_0|$, to avoid possible SNR degradation, the proper choice of $T_\Delta f_s$ is essential.

$$|C| = |1 - \beta^{\pm nd}| = \sqrt{2 \cdot \{1 - \cos[2\pi T_\Delta f_S |nd|]\}}, \quad nd = n_1 \pm n_0. \tag{12}$$

Although the level of the desired signal is increased by optimizing T_Δ, it can cause the side effect of a large group delay if T_Δ is too large. There are two solutions to compensate for this group delay effect [11]. First, an interpolator following the stream B interpolant can be resampled to align two streams in the time domain. Another method is to modify the frequency response of the stream B interpolant by subtracting the group delay effect of $2\pi T_\Delta f_0$. A modified response of the stream B interpolant is expressed by

$$S_{B(com)}(f) = S_B(f) \cdot e^{j2\pi T_\Delta f_0}. \tag{13}$$

3. Second-Order BPS FE for Three-Band Signals

We introduce a method to receive more than two-band RF signals simultaneously and separate each of them under the precondition that three band-pass RF signals lie in the n_0, n_1, and n_2 frequency zones. The spectra in the positive axis are shown in Fig. 8. The spectra of the three signals are defined as $R^0(f)$, $R^1(f)$, and $R^2(f)$. Signals aliased from each zone have different phase shifts in stream B as shown in Fig. 8. As discussed in section II, $[0, f_s/2]$ contains all the signals we

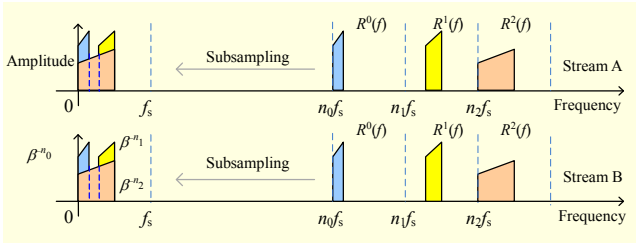

Fig. 8. Spectrum and relative phase of three-band RF signals.

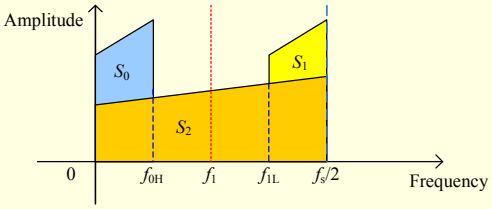

Fig. 9. Three-band signals after BPS within $[0, f_s/2]$.

want to receive. We defined the three signals in $[0, f_s/2]$ as S_0, S_1, and S_2 as shown in Fig. 9.

We define f_1 as the middle of S_0 and S_1, that is

$$f_1 = f_{0H} + (f_{1L} - f_{0H})/2, \tag{14}$$

where f_{0H} is the highest frequency of signal S_0, and f_{1L} is the lowest frequency of signal S_1.

As seen in Fig. 9, in $[0, f_1]$ only S_0 and S_2 are overlapped, and in $[f_1, f_s/2]$ only S_1 and S_2 are overlapped. If we want to separate S_0 and S_1 from S_2, we simply remove S_2 by using the interpolants we designed in section III as

$$S_{A1}(f) = \begin{cases} 1/B, & |f| < B, \\ 0, & \text{otherwise}, \end{cases} \tag{15}$$

$$S_{B1}(f) = \begin{cases} -\beta^{-n2}/B, & -B < f < 0, \\ -\beta^{n2}/B, & 0 < f < B, \\ 0, & \text{otherwise}. \end{cases} \tag{16}$$

Then, after filtering using interpolants $S_{A1}(f)$ and $S_{B1}(f)$ the outputs have only S_0 and S_1 remaining. As these two signals do not overlap each other, they can be separated using proper filters.

A low-pass filter is defined as

$$S_{LP} = \begin{cases} 1, & [0, f_1], \\ 0, & \text{others}. \end{cases} \tag{17}$$

It is used to remove S_1 from S_0. A high-pass filter is defined as

$$S_{HP} = \begin{cases} 1, & [f_1, f_s/2], \\ 0, & \text{others}. \end{cases} \tag{18}$$

It is used to remove S_0 from S_1. Then, after filtering using

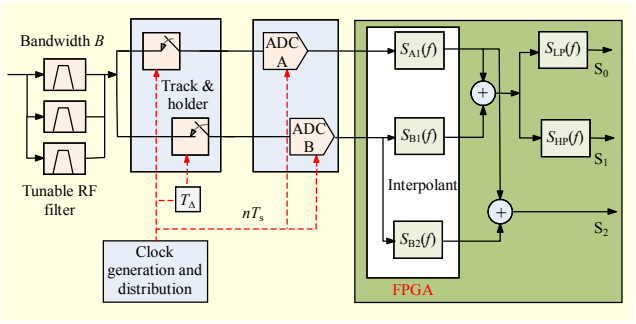

Fig. 10. Architecture of three-band access second-order BPS receiver.

interpolants and two filters, S_0 and S_1 are separated.

If we want to separate S_2 from S_0 and S_1, we design interpolants to remove S_0 from $[0, f_1]$ and to remove S_1 from $[f_1, f_s/2]$.

Thus, an interpolant is defined as

$$S_{A2}(f) = S_{A1}(f) = \begin{cases} 1/B, & |f| < B, \\ 0, & \text{otherwise}, \end{cases} \tag{19}$$

$$S_{B2}(f) = \begin{cases} -\beta^{-n_1}/B, & -f_s/2 < f < -f_1, \\ -\beta^{-n_0}/B, & -f < f < 0, \\ -\beta^{n_0}/B, & 0 < f < f_1, \\ -\beta^{n_1}/B, & f_1 < f < f_s/2, \\ 0, & \text{otherwise}. \end{cases} \tag{20}$$

The architecture of the proposed three-band access BPS receiver is shown in Fig. 10. Three tunable RF filters select signals received simultaneously. The reconfigurable interpolants suppress overlapped signals. Low-pass and high-pass filters are used to separate signals in different frequencies.

IV. Implementation of BPS FE and Performance Test

We introduce the second-order BPS FE to verify the features described in sections II and III. We designed a receiver platform based on BPS FE to verify the performance of the band-pass sampling system proposed in section III. It is very hard to find commercial ADCs that operate at a moderate sampling rate with low power consumption and have a very wide analog bandwidth of up to 5 GHz. In our design, a conventional IF sampling purpose ADC is preceded by a gigahertz track and holder (T&H). Two wide-band T&H chips are proposed to subsample band-pass RF signals and perform frequency down-conversion to the baseband. The ADC chip is proposed to be used as a quantizer. The analog bandwidth of the T&H must be larger than the maximum frequency of the RF signal, whereas the quantizers operate at a rate of $2B$ (B is

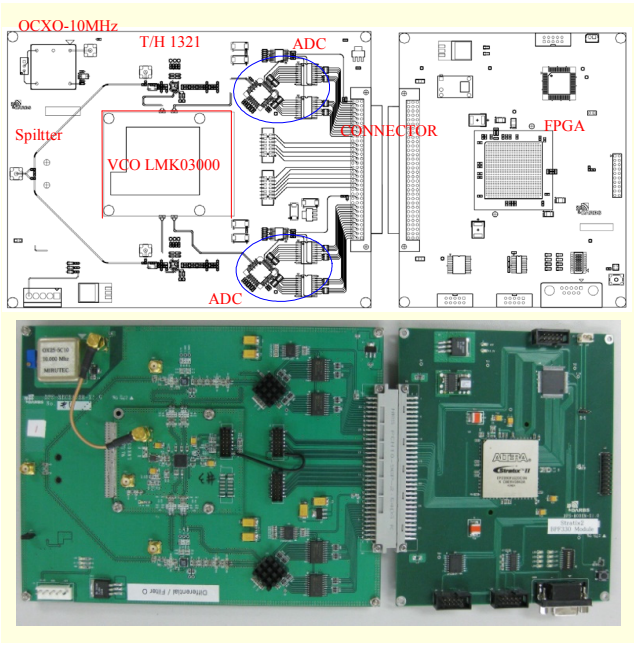

Fig. 11. Second-order BPS FE platform.

the bandwidth of the RF tunable filter). The clock generator block is responsible for distribution of a stable clock to the T&H, ADC, and FPGA, with an extremely low jitter, which also generates different time delay between two ADC paths, that is, T_Δ. Figure 11 shows the second-order BPS FE platform that was implemented in this research.

1. Performance Verification of Two-Band Signal

We demonstrated two-band access features enabled by employing the proposed second-order BPS FE. In this test, RF signals were subsampled at a rate of 60 MHz and the largest delay of 2,250 ps was used. It was preconditioned that each channel could access four different bands respectively as shown in Fig 12. Also, we could choose one of 16 sets of interpolants according to the combination of band positions.

We show one of the test results when a 4-QAM signal centered at 2.404 GHz (n_0=40) and an AM signal centered at 1.264 GHz (n_1=21) were received simultaneously. Some

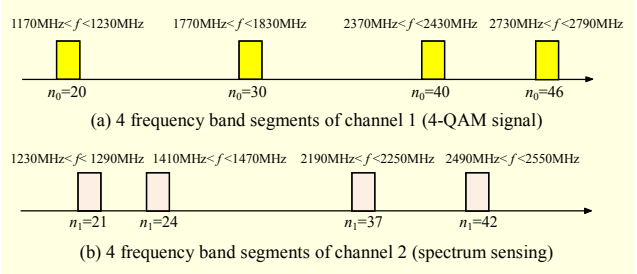

Fig. 12. Example band positions.

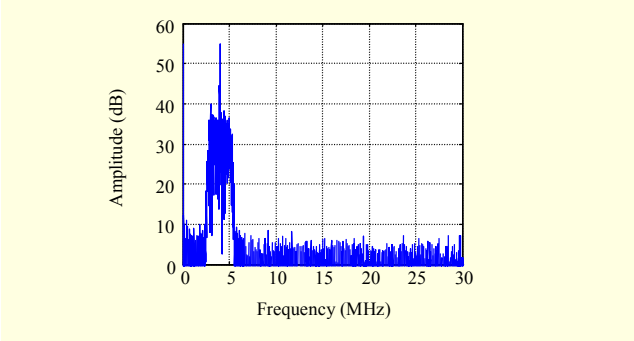

Fig. 13. FFT of ADC output samples.

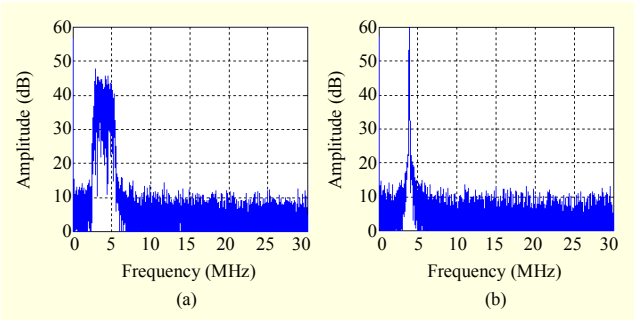

Fig. 14. FFT of separated signals: (a) 4-QAM from 2.404 GHz and (b) AM from 1.264 GHz.

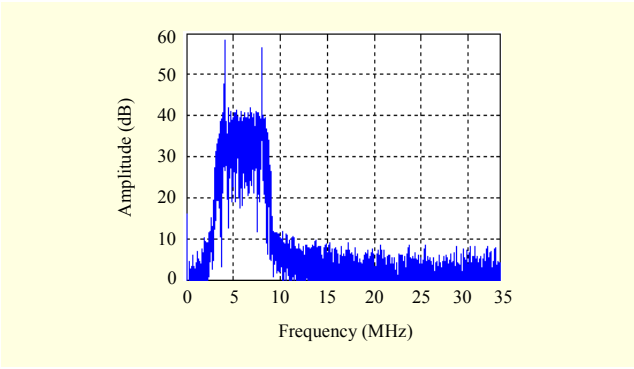

Fig. 15. FFT of ADC output samples.

sample streams were captured from an FPGA to generate an FFT or scattered plot. Figure 13 shows the FFT of the output of the ADC in which two signals are overlapped. The two signals are separated by applying the interpolant described in (6), (10), and (11). The FFTs of the two separated signals are depicted in Fig. 14.

2. Performance Verification of Three-Band Signal

In this study, RF signals were subsampled at a rate of 66.67 MHz, and a delay of 1,950 ps was used. We show one of the test results when a 4-QAM signal centered at 1.3393 GHz (n_0=20), an AM signal centered at 1.0707 GHz (n_1=16), and an

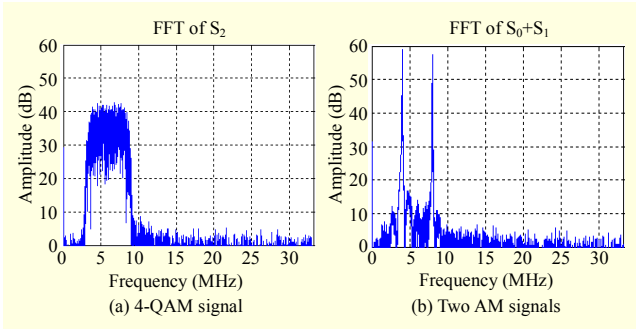

Fig. 16. FFT of separated signals.

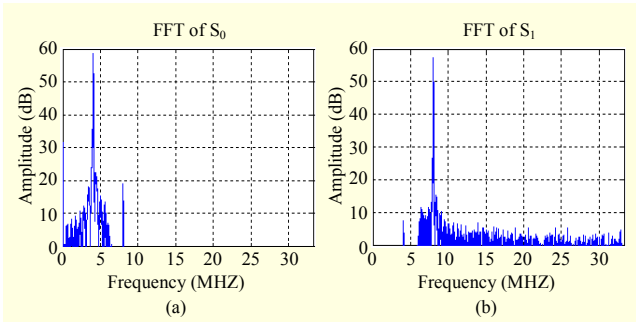

Fig. 17. FFT of separated AM signals.

AM signal centered at 1.608 GHz (n_2=24) were received simultaneously. Figure 15 shows the FFT of the output of the ADC in which 4-QAM signals overlapped with two AM signals. By applying the interpolant described in (19) and (20), two AM signals from different frequencies were suppressed simultaneously as shown in Fig. 16(a). By applying the interpolant described in (15) and (16), 4-QAM signals were suppressed as shown in Fig. 16(b). Figure 17 shows the FFTs of the AM signals separated by low-pass and high-pass filters described in (17) and (18), respectively.

V. Conclusion

We proposed a frontend architecture based on second-order BPS particularly for CR and SDR systems which provides flexibility in accessibility to a wide range of frequency regions. This BPS receiver can access or scan any frequency band without limitation in frequency band position. It also down-converts multiband signals simultaneously and separates signals by suppressing mutual interference using digital signal processing. This proposed BPS FE architecture also enables a CR system to perform environment sensing for unused frequency segments on the normal receiving operation. To verify and demonstrate the usefulness of the proposed BPS FE, a hardware platform was implemented and test results were presented. We expect that the BPS-FE-based receiver will

operate well in practical application.

References

[1] A. Willig, "Recent and Emerging Topics in Wireless Industrial Communications: A Selection," *IEEE Trans. Ind. Informat.*, vol. 4, no. 2, May 2008, pp. 102-124.

[2] S. Haykin, "Cognitive Radio: Brain-Empowered Wireless Communications," *IEEE J. Sel. Areas in Commun.*, vol. 23, no. 2, Feb. 2005, pp. 201-220.

[3] M.Y. Kim and S.J. Lee, "Design of Dual-Mode Digital Down Converter for WCDMA and cdma2000," *ETRI J.*, vol. 26, no. 6, Dec. 2004, pp. 555-559.

[4] N. Vun and A. Premkumar, "ADC Systems for SDR Digital Front-End," *Proc. Ninth Int. Symp. Consumer Electron. (ISCE)*, 2005, pp. 359-363.

[5] T. Fujii, Y. Kamiya, and Y. Suzuki, "Multi-Band Ad-Hoc Cognitive Radio for Reducing Inter System Interference," *IEEE 17th Int. Symp. Personal, Indoor and Mobile Radio Commun.*, Sept. 2006, pp. 1-5.

[6] K. Jones et al., "Holistic Systems Engineering: Cognitive Hierarchy, RF Receiver Technology, and Environment," *25th IEEE/AIAA Digital Avionics Systems Conf.*, Oct. 2006, pp. 1-11.

[7] J. Mitola, "The software radio architecture," *IEEE Communications magazine*, vol. 33, no. 5, May 1995, pp.26-38.

[8] S. Rodriguez-Pareram et al., "Front-End ADC Requirements for Uniform Bandpass Sampling in SDR," *Proc. VTC2007-Spring, IEEE 65th Vehicular Technol. Conf.*, Apr. 2007, pp. 2170-2174.

[9] R.G. Vaughan, N.L. Scott, and D.R. White, "The Theory of Bandpass Sampling," *IEEE Trans. Signal Process.*, vol. 39, no. 9, Sept. 1991, pp. 1973-1984.

[10] J.H. Kim et al., "The Analysis and Design of RF Sub-Sampling Frontend for SDR," *Int. Workshop on Cognitive Network and Commun.*, Hangzhou, China, Aug. 2008.

[11] S.S. Myoung, Y.H. Kim, and J.G. Yook, "Impact of Group Delay in RF BPF on Impulse Radio Systems," *IEEE MTT-S Int. Microw. Symp. Digest*, vol. 4, June 2005, pp. 1891-1894.

HyungJung Kim received the BS and MS degrees in electronics engineering from Hanyang University, Seoul, Korea, in 1992 and 1994, respectively. Since 1995, he has been with ETRI. He has researched in the fields of the wireless communication systems and digital signal processsing. His recent interests include digital RF, software defined radio, and cognitive radio technologies.

Jin-up Kim received the BS degree from Korea University, Seoul, Korea, in 1985, and the MS and PhD degrees from Korea Advanced Institute of Science and Technology, Seoul, Korea, in 1987 and 1996, respectively. He has been with ETRI since 1987. He has also been a professor of the University of Science and Technology in the field of wireless communications since 2005. He has researched in the field of the wireless communication systems. His recent interests include digital RF, software defined radio, and cognitive radio technologies.

JaeHyung Kim received his BS and MS degrees in electronics engineering from Korea University, Seoul, Korea, in 1983 and 1985, respectively. He received the PhD in communication engineering from Korea University in August, 1989. Since 1991, he has been with Changwon National University, where he is currently a professor of the School of Mechatronics Engineering. His current research interests include wireless modem design and implementation, specifically focused on RF sampling digital signal processing for SDR. He is currently a member of the IEEE.

Hongmei Wang received the BS degree in automation control engineering from Qingdao University, China, in 2006. She is currently studying with the School of Mechatronics Engineering, Changwon National University, Korea, for the MS degree. Her research interests include systems applied to wireless communication modems and various systems required for advanced digital signal processing.

InSung Lee received the BE and ME degrees in electronics engineering from Yonsei University, Korea, in 1983 and 1985, respectively. He received the PhD in electrical engineering from Texas A&M University in 1992. He worked for ETRI from 1993 to 1995. He was involved in a project developing CDMA and a mobile communication system at ETRI. Since Oct. 1995, he has been with the School of Electrical, Electronics and Computer Engineering, Chungbuk National University, Korea. He has conducted research in the areas of speech and audio coding, data compression, mobile communication, and signal processing for communication. He is currently a member of the IEEE, KICS, IEEK, and ASK.